

Nonlinear analysis of RC frames considering shear behaviour of members under varying axial load

J. Shayanfar¹ · H. Akbarzadeh Bengar¹

Received: 27 February 2016 / Accepted: 29 November 2016 / Published online: 16 December 2016
© Springer Science+Business Media Dordrecht 2016

Abstract In this paper, the role of shear failure in the seismic behaviour of reinforced concrete structures has been investigated. In current practice, the effects of shear on beams and columns are usually neglected in nonlinear analysis, which is carried out based on the flexural behaviour of each element. In such analyses, only the flexural behaviour of the member is considered, while the experimental results confirmed the possibility of other modes failure prior to ultimate flexural capacity. Also, it is now generally accepted that axial load plays a dominant role in evaluating the seismic behaviour of RC columns. However columns, especially the exterior ones, can be subjected to variable axial loads depending on the lateral loads. In this study, a numerical model including rotational springs, was developed to simulate the effects of shear for beams and columns based on the material failure mechanism. Moreover, a procedure was recommended to take into account the effects of the variations of axial load on RC columns. In order to verify the proposed model for columns, the obtained results of the analytical analysis were compared to experimental results. The results predicted by the proposed model were in good agreement with the experimental tests. In addition, to evaluate the performance of the proposed model at structural level, two RC frames with various failure modes have been investigated and the results confirmed the ability of the model in predicting the inelastic behaviour of the frame, which can provide an alternative method in current practice. Moreover, a parametric analysis were carried out in order to highlight the effect of the variations of axial load on nonlinear response of reinforced concrete columns.

Keywords Analytical model · Shear failure · Axial load variations · Non-linear static (pushover) analysis · RC column

✉ H. Akbarzadeh Bengar
h.akbarzadeh@umz.ac.ir

¹ Department of Civil Engineering, University of Mazandaran, Babolsar, Iran

1 Introduction

Reinforced concrete (RC) structures may have a high seismic vulnerability during seismic actions. The inadequate shear capacity of columns can be one of the most severe deficiencies of such structures which make them vulnerable against earthquakes. Experimental, numerical and analytical studies (Aboutaha et al. 1999; Lynn 2001; Sezen 2002; Ousaleem et al. 2002; Sezen and Moehle 2002; Elwood and Moehle 2003; Colajanni et al. 2015; Ousaleem et al. 2003; Elwood 2004; Elwood and Moehle 2005; Baradaran Shoraka 2013) as well as post-earthquake reconnaissance confirmed that failure mode of RC columns in existing structures with inadequately and light detailed transverse reinforcement may be shear failure, and consequently, axial failure. Moreover, experimental studies (Ang et al. 1989; Aschheim and Moehle 1992; Wong et al. 1993; Ho and Pam 2003; Lee and Watanabe 2003; Moretti and Tassios 2007; Mullapudi and Ayoub 2010) confirmed that the shear capacity of columns is significantly dependent on their inelastic flexural deformations. Several models for shear have been provided to compute the reduction of shear-capacity of RC members. The ATC (1996) seismic design guideline developed a model for describing the interaction between shear capacity and displacement ductility demand. Priestley et al. (1994) provided a shear-capacity model for RC columns by taking into account the shear strength due to concrete, transverse reinforcement, and axial load. Sezen and Moehle (2004) proposed a new model for predicting the column shear capacity based on theoretical formulations and experimental evidence. Based on this model, the shear capacity contribution due to concrete is related to displacement ductility demand. According to the material failure criteria of concrete, Park et al. (2006) developed a theoretical model to estimate the shear capacity of slender RC beams without transverse reinforcement. Since the normal stresses distribution changes due to the beam inelastic flexural deformation, the shear capacity was computed as a function of the flexural deformation. Park et al. (2012) used a similar approach to predict the shear-capacity degradation and the deformation capacity of slender RC columns subjected to cyclic lateral loading.

On the other hand, experimental studies conducted by Lynn (2001), Sezen (2002) and Matchulat (2009) proved that the axial load largely affects the response of members in terms of the load–deflection and the mode of failure. Also, RC columns with high axial load ratios result in sudden, brittle failures than RC columns under lower axial load ratios. Regarding the effects of variations of axial load on the nonlinear behaviour of columns, Kreger and Linbeck (1986), Abrams (1987), Li et al. (1988), Lynn (2001), Ousaleem et al. (2002) and Sezen (2002) performed tests on RC columns under varying axial load. The observed response of the RC columns in terms of the strength, deformation capacity and stiffness was significantly different from those columns subjected to reversals of lateral load under constant axial load. Moreover, Saadeghvaziri and Foutch (1990) investigated the effect of vertical ground motion on the dynamic response of Highway Bridge. Vertical motion induces a change in the axial load in the columns. This analytical study demonstrated that hysteresis loops of columns and piers are very asymmetric and unstable, leading to uncoupled variations in the axial load. They found a significant fluctuation in the strength and stiffness of the columns. For the analysis of the hysteretic response of RC columns subjected to varying axial load, Taucer et al. (1991) proposed a new fiber beam-column finite element along with a consistent nonlinear solution algorithm. ElMandooh Galal and Ghobarah (2003) proposed an inelastic biaxial model based on plasticity theory.

This quadri-linear degrading model considers the effect of variations of axial load on lateral deformation.

Some model have been proposed in literature to obtain the nonlinear response of RC columns during shear and axial load failure. Elwood and Moehle (2003) provided a shear-friction model based on the observation from experimental tests to calculate the drift ratio at axial failure of a shear-damaged column. Elwood (2004) proposed a uniaxial material model that incorporates the failure surfaces and the subsequent capacity degradation. Moharrami et al. (2015) used nonlinear truss models to capture nonlinear response of shear-dominated RC columns subjected to cyclic loading. The concrete constitutive equations were modified to account for the contribution of the aggregate interlock to the shear strength.

To estimate the nonlinear behavior of a RC column subjected to varying axial load, the existing models in literature are generally not practical and simple enough to be adopted in commercial nonlinear analysis softwares. Therefore, providing a simplified but accurate model is required. Also, the model should consider the effect of variations of axial load to capture the realistic and complete response of columns as well as structures.

In this study, in order to consider the shear effect in members, a model was suggested, where the nonlinear behaviour of members was simulated by rotational springs. To evaluate the properties of the spring, the seismic shear behavior was computed based on material failure mechanism. For this purpose, shear effect was implemented in the flexural moment–rotation curve of the member. Moreover, a procedure was proposed for considering the effects of axial failure mechanism and variations of applied axial load to columns.

2 Numerical model

In order to evaluate the nonlinear behaviour of RC structures using a lumped plasticity model, the calculation of plastic hinge properties is needed. Considering only the flexural nonlinear behaviour of structural components with common assumption that shear behaviour of members can be simplified and neglected in nonlinear analyses, misleading results in terms of the prediction of the performance of structures can be obtained (Guner and Vecchio 2011). Therefore, flexural and shear inelastic behaviours of the structural components should be considered in calculation of properties of plastic hinges. To simulate this behaviour, a numerical model with rotational springs in beam and column was proposed as shown Fig. 1. L is the distance of critical section to the point of contraflexure. L_p is the plastic hinge length, evaluated according to Paulay and Priestley (1992). The other dimensions are described in figure. It should be noted that in an accurate numerical model, consideration of nonlinearities in the joint panel is required. However, some past studies (Niroomandi et al. 2010, 2014; Shayanfar and Akbarzadeh 2016; Shayanfar et al. 2016) indicated that for RC structures with adequate transverse reinforcements in the joint panel, the shear demand induced by seismic actions is significantly lower than the shear capacity. Therefore, diagonal cracking in the joint panel does not occur.

In practical applications, the numerical model can be useful to analyze members as well as structure using commercial software programs. Therefore, the determination of the accurate properties of these springs is necessary.

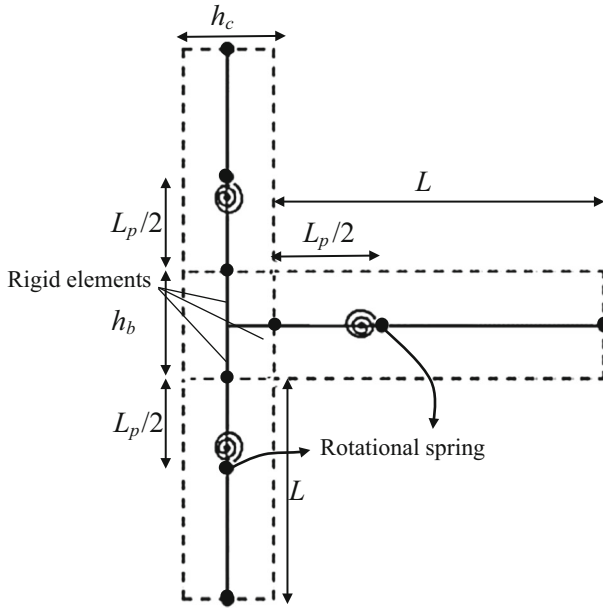


Fig. 1 Plastic hinge locations at the RC members for a typical exterior joint

3 Flexural and shear effects in beam and column

Different failure modes in beams and columns can be detected comparing shear capacity and shear demand. According to the proposed model, these failures are detected by using rotational spring. In order to calculate the properties of the rotational springs, moment–curvature analysis of section is required based on the principles of strain compatibility and equilibrium and material constitutive relations for concrete and steel (see Fig. 2). Here, ϵ_c and c define the value of concrete strain at the extreme compression fiber and the value of neutral axis depth, respectively. The other parameters are described in figure. In a RC member confined by transverse reinforcements, the confinement effect should be considered in the stress–strain characteristics of concrete.

In the present study, the Mander et al. (1988)’s stress–strain model was used for unconfined and confined concrete, adopted for concrete of core and cover of section,

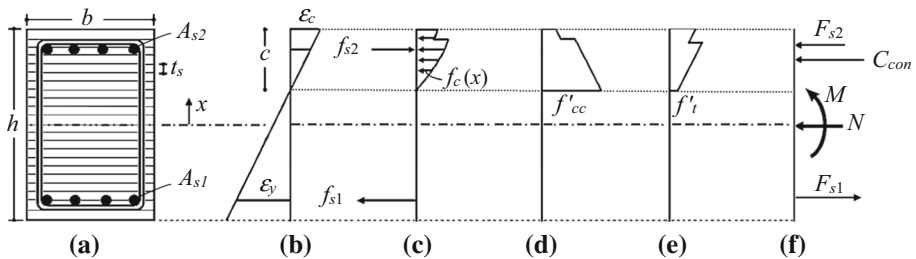


Fig. 2 Layer-by layer sectional analysis of a RC section: **a** cross-section, **b** normal strain distribution, **c** normal stress distribution, **d** shear stress capacity of concrete controlled by compression, **e** shear stress capacity of concrete controlled by tensile and **f** forces

respectively. The elastic–plastic model was considered for steel bars. Once the moment–curvature curve of section is formulated, it can be converted into moment–rotation curve considering the curvature distribution along the member length. However, the shear effect in member should be considered in the calculation of moment–rotation curve, following the iterative procedure given below:

1. Assume a value of concrete strain, ϵ_c , at the extreme compression fiber.
2. Assume a value of neutral axis depth, c .
3. Compute the total compressive force in concrete, C_{con} , and the compressive and tensile forces, F_{si} , in longitudinal reinforcements as follows

$$C_{con} = \sum f_c(x)b t_s \tag{1}$$

$$F_{si} = \sum f_{si}A_{si} \tag{2}$$

where t_s is the strip thickness in the cross section; b is the member width; A_{si} is the area of longitudinal reinforcements at the i -th re-bar layer; x is the distance from the centroidal axis.

4. Check the force equilibrium [Eq. (3)]. If $C_c + F_{si}$ is closed to the applied axial force, then the assumed value of c is correct and go to step 5. Otherwise assume a new value of c and go to step 2.

$$C_c + F_{si} - N = 0 \tag{3}$$

5. Compute the bending moment, M_f , as follows

$$M_f = \sum f_c(x)bt_sx_i + \sum F_{si}\left(\frac{h}{2} - d_i\right) \tag{4}$$

6. Calculate the equivalent shear moment, M_s , corresponding to the normal stress, $f_c(x)$, as follows

$$M_s = V_n \times L \tag{5}$$

In Eq. (5), L is the distance of critical section to the point of contra-flexure; V_n is the shear strength of the member taking into account the contributions of concrete and transverse reinforcements, calculated by Eq. (6) as follows

$$V_n = \sum v(x)bt_s + \frac{A_vf_{yv}d}{s} \tag{6}$$

where A_v is the total transverse reinforcement area; f_{yv} defines the yielding strength of the transverse reinforcements; s is centre to centre spacing of transverse reinforcement; $v(x)$ is the concrete shear stress acting on the cross section corresponding to the normal stress $f_c(x)$ that can be computed using the approach developed by Park et al. (2006, 2012). It is well known that a RC member is subjected to opposite sign moments at its ends during seismic loads. It can induce

the tension and compression zones in the cross-section. Therefore, as shown in Fig. 3, an element of the beam or column section is subjected to the shear stress and the compressive normal stress. According to resulted principal compression and tension stresses, crushing or diagonal cracking of the concrete may appear in the member (if flexural capacity is more than shear capacity). Based on the Rankine’s failure criteria (Chen 1982), the failure of materials can occur when the principal compression and tension stresses induced by the combined stresses reaches the strength of materials. Therefore, by taking into account the interaction between the principal compression and tension stresses and the compressive normal stress, based on Mohr’s circle approach, the shear capacity in an element of the section can be written as

$$v_c(x) = \sqrt{f'_{cc} [f'_{cc} - f_c(x)]} \quad \text{failure controlled by compression} \quad (7)$$

$$v_c(x) = \sqrt{f'_t [f'_{cc} - f_c(x)]} \quad \text{failure controlled by tension} \quad (8)$$

$$v_c(x) = \sqrt{f'_t [f'_{cc} - f_c(x)]} \quad (9)$$

where f'_t denote the tensile strength of concrete which can be taken into account as (MacGregor et al. 1960)

$$f'_t = 0.292 \sqrt{f'_c} \quad (10)$$

As a result, the total shear capacity of a RC member can be determined in terms of the sum of the shear capacities due to the concrete contribution, $\sum v(x)$, and

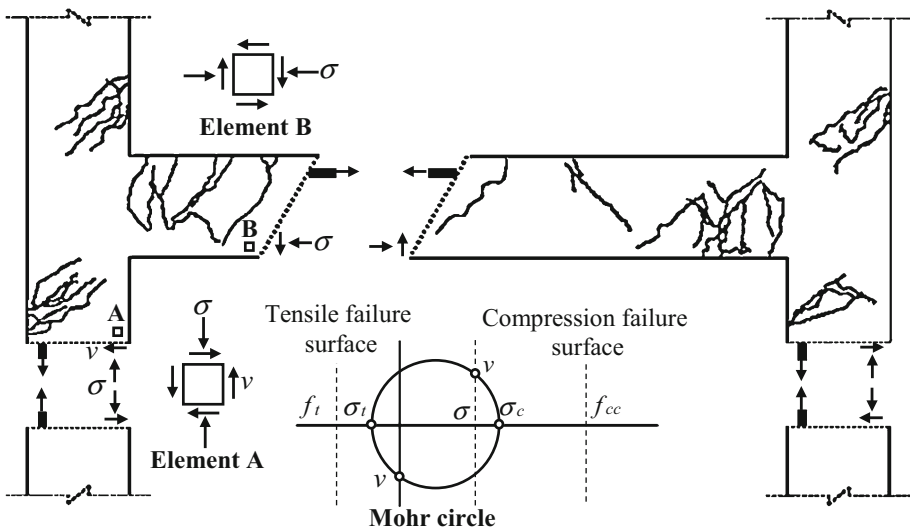


Fig. 3 Rankine’s failure criteria (Chen 1982) for concrete

the transverse reinforcement contribution [Eq. (6)]. It should be noted that if compressive strain in concrete is higher than strain at the peak compressive strength of unconfined and confined concrete, $v_c(x)$ is considered equal to zero. In other words, at a compressive fiber where the concrete stress reaches the compressive strength of the concrete, the contribution of the concrete can be neglected due to the fact that crushing occurs in the concrete and principle compressive stress reaches the failure surface (see Fig. 3). Therefore, the concrete in the compressive fiber cannot develop any shear capacity (Park et al. 2006). According to Willams and Sexsmith (1995) and Park et al. (2012), the deformation capacity was taken into account as the deformation corresponding to 80% of the strength in the intersection of the shear demand and shear capacity curves. In current study, it was assumed that (1) the compression zone of the intact concrete provides the shear capacity of beam or column (to be conservative and simple); and (2) the effect of aggregate interlock and dowel action is ignored (nearly correct if the longitudinal reinforcement has yielded due to the fact that the tensile zone in the cross-section of RC columns is significantly damaged by flexural cracking). Therefore, the shear capacity of intact concrete in the compression zone is severely greater than the contributions of the dowel action and aggregate interlock (Park et al. 2006, 2012).

7. Determine the moment carrying capacity as follows

$$M = \min(M_b, M_s) \tag{11}$$

8. Calculate the rotation corresponding to M as follows:

$$\theta_i = \frac{\varphi_i L_{eff}}{2} \quad \text{for } \varepsilon_s \leq \varepsilon_y \tag{12}$$

$$\theta_i = \theta_y + (\varphi_i - \varphi_y) L_p \quad \text{for } \varepsilon_s \geq \varepsilon_y \tag{13}$$

in which (Paulay and Priestley 1992)

$$\varphi_i = \frac{\varepsilon_c}{c} \tag{14}$$

$$L_{eff} = L + 0.022 f_s d_b \quad f_s \leq f_y \tag{15}$$

$$L_p = kL + 0.022 f_y d_b \geq 0.044 f_y d_b \tag{16}$$

$$k = 0.2 \left(\frac{f_{su}}{f_y} \right) - 1 \leq 0.08 \tag{17}$$

where f_{su} is the ultimate stress of the steel.

9. Repeat steps 1–8 for a range of ε_c . Maximum value of ε_c can be calculated based on ultimate strain in the extreme compression fiber of concrete core,
10. Plot moment–rotation curve.

Following the above steps, the moment–rotation characteristics of rotational springs can be determined. Figure 4 shows interaction between shear and flexural behaviours using the developed shear model. As can be seen, failure mode of RC beams and columns can be considered in three different categories including flexural, shear–flexural and shear failure which are detected by comparing the values of shear and flexural moments.

In this study, the slope of moment–curvature curve prior to reaching yield moment is used as the effective flexural stiffness in nonlinear analysis. It is described by Eq. (18):

$$E_c I_{eff} = \frac{M_y}{\varphi_y} \tag{18}$$

In Eq. (18), M_y defines the yield moment at critical section. E_c is the modulus of elasticity of concrete.

In current paper, the evaluation of reinforcement buckling limit state was taken into account following the methodologies of the recommended by Berry and Eberhard (2005). According to the mentioned model, the plastic rotation at the onset of buckling can be computed as:

$$\theta_{p_bb} = C_0 \left(1 + C_1 \rho_{eff} \right) \left(1 + C_2 \frac{N}{A_g f'_c} \right)^{-1} \left(1 + C_3 \frac{L}{h_2} + C_4 \frac{f_y d_b}{h_2} \right) \tag{19}$$

in which

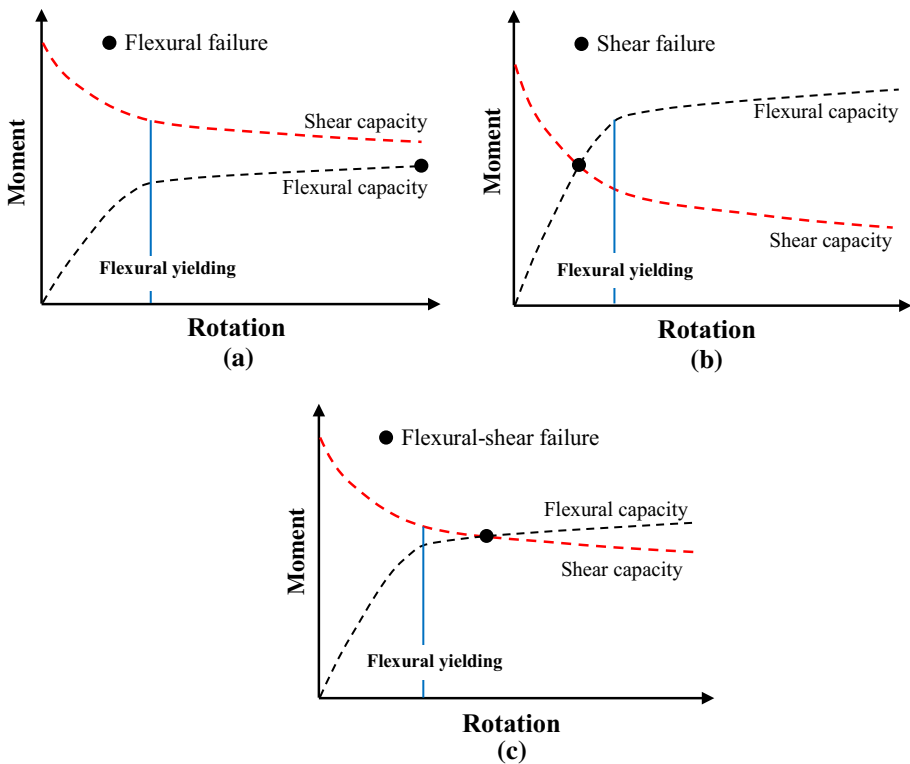


Fig. 4 Interaction between shear and flexural capacities of RC members with **a** flexural behaviour; **b** shear behaviour; **c** shear–flexural behaviour

$$\rho_{eff} = \frac{f_{yv}}{f_c} \rho_s \quad (20)$$

where C_0 , C_1 , C_2 , C_3 and C_4 were taken into account as 0.019, 1.65, 1.797, 0.012 and 0.072, respectively; ρ_s denotes the volumetric ratio of the transverse reinforcements. Finally, rotation at the onset of bar buckling can be obtained by:

$$\theta_{bb} = 1.07 \frac{\varepsilon_y}{h} L + \theta_{p_bb} \quad (21)$$

As a result, ultimate rotation of a RC member can be controlled by using the aforementioned criteria. It should be noted that Berry and Eberhard (2005) adopted the Priestley et al. (1996)'s model to approximately estimate the yield curvature ($\varphi_y = 2.14 \times \varepsilon_y/h$). Therefore, in Eq. (21), this model was considered to determine the yield rotation. Moreover, the study conducted by Niroomandi et al. (2015) proved the reliability of the method recommended by Berry and Eberhard (2005).

It is noteworthy that if shear failure occurs in columns, axial failure mechanism becomes the critical parameter based on the studies conducted by Lynn (2001), Sezen (2002), Ousalem et al. (2002), Elwood (2004), Elwood and Moehle (2005) and Baradaran Shoraka (2013), such that columns axial capacity will lose. The relationship between applied axial load on column and the drift at axial failure (Δ_a/L) can be determined as (Elwood and Moehle 2005);

$$\frac{\Delta_a}{L} = \frac{4}{100} \frac{1 + \tan^2 65^\circ}{\tan 65^\circ + N\left(\frac{s}{A_{sv} F_{yv} d_c \tan 65^\circ}\right)} \quad (22)$$

where 65° and d_c represent the assumed angle of the shear failure plane and the depth of the column core, respectively. Therefore, for a given axial load, the column horizontal drift or displacement in axial failure can be derived. On the other hand, after detection of axial failure, according to the extracted results of tests conducted by Lynn (2001), Sezen (2002), Ousalem et al. (2002) and Elwood and Moehle (2003) also the reported results from analytical study by Elwood (2004), an increase in lateral shear deformations can lead to an increase in axial deformations and a reduction in axial load capacity. Therefore, shear–axial interaction should be considered. For this purpose, the model provided by Elwood (2004) is not simplified enough to be used in existing commercial softwares. This model needs a special purpose program for simulating shear–axial interaction. In this paper, a simplified analytical procedure was provided to take into account shear–axial interaction. Figure 5 shows interaction between shear moment, rotation and axial load for shear-damaged columns with axial failure (type 1) and with no axial failure (type 2). Here, θ_b and θ_c denote the column rotation at 80% of maximum shear moment, M_i . As can be seen in Fig. 5, for the column type 1, the axial strength demand corresponding to column rotation, θ_b , (point B) is higher than the axial capacity of the column. In this case, θ_a (point A) is assumed as the ultimate rotation corresponding to the formation of axial mechanism at 30% of maximum shear moment. Using this procedure, not only the effect of the column axial failure was considered but the column post peak behaviour was also modified. However, for column type 2, when the column rotation reaches point C, the axial capacity corresponding to the column rotation, θ_c , is higher than the axial strength demand of the column. In this case, the no axial mechanism would appeared in the column.

4 Effect of variations of applied axial load

This section describes the effect of variations of axial load on nonlinear behaviour of columns in RC frame. It is now generally accepted that axial load plays a dominant role in evaluating the seismic behaviour of the column. However columns, especially the exterior ones, can be subjected to variable axial loads due to the lateral loads. Under seismic loading, lateral inertial forces generate overturning moments. These moments are converted into axial load in the column, tensile on one side of the frame and compressive on the opposite. Properties of a RC column, namely crack stresses, instantaneous rigidities, and yield stresses due to fluctuations of axial loads during seismic actions. For example, for a RC column at the tensile side, concrete cracking occurs earlier and the column strengths and rigidities may decrease. Therefore, when axial compression reduces, columns behave much softer than columns under constant axial load levels. In these columns, axial compression decreases and the neutral axis location is translated towards the extreme compressive fibre of section. Subsequently, the effective area of the cracked section decreases and resisting flexural demand is derived with less material. On the other hand, when axial compression increase, the neutral axis location is translated towards the extreme tensile fibre of section. The relation between the axial load and the column shear force or the column moment can be repressed as:

$$N = N_g \pm KV_n = N_g \pm K \frac{M}{L} \tag{23}$$

where K is the axial load factor. According to above discussion, it is clear that axial load is one of the most important parameters in the calculation of moment–rotation of columns. Therefore, increase or decrease of axial load during seismic action can significantly influence the nonlinear behaviour of columns. In order to calculate the axial load factor, a

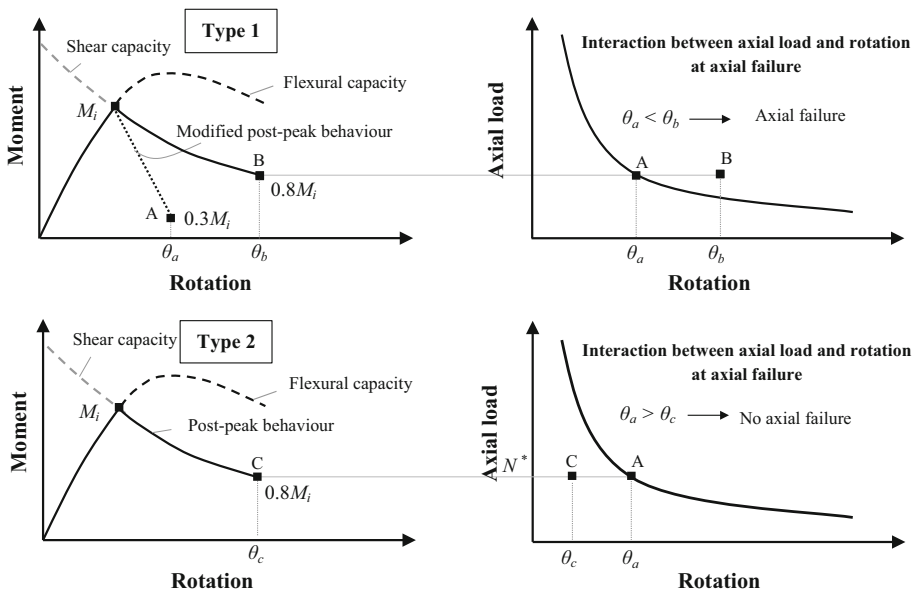


Fig. 5 Moment–rotation relation by considering shear–axial load interaction

preliminary pushover analysis of the RC frame system is required (computing the ratio of the applied axial load on column due to lateral loads to the column shear force). To determine the linear relationship between axial load and inter-storey shear of column, a simplify procedure was developed as given below:

1. Perform static nonlinear analysis for a predefined distribution of horizontal loads.
2. Determine the relationship between column axial load and column shear force for each step loading.
3. Plot column axial load-column shear force.
4. Compute a linear regression analysis of column axial load on obtained column shear force from pervious step.
5. Calculate proportion coefficient value of K .

Using this parameter, total applied axial load on, N , due to an induced axial force in column, $\Delta N = K \times V_c$, and gravity load can be derived.

Traditionally, this effect can be simulated by defining axial-moment hinge at ends of columns. Axial-moment hinge can be defined by axial load–moment interaction diagram. Moreover, for each axial load level, moment–rotation relation is determined to define complete inelastic behaviour of column. This method works well only for columns with flexural failure since the shear capacity of column is more than flexural capacity in such cases. However, for columns with shear or flexural–shear behaviour, we need to modify Eq. (3), since the neutral axis location is varied by fluctuating axial loads during lateral loading. According to Eq. (23), for determining shear and flexural capacities considering the effects of variations of axial load, the natural axis can be calculated by Eqs. (24) and (25), respectively.

$$\sum f_c(x)b_w t_s \left(1 - \frac{K}{L} x_i\right) + \sum F_{si} \left(1 - \frac{K}{L} \left[\frac{h}{2} - d_i\right]\right) = N_g \quad \text{for } M_b \leq M_s \quad (24)$$

$$\sum f_c(x)b_w t_s + \sum F_{si} - K \sum v(x)b_w t_s - K \frac{A_v f_{yv} d}{s} = N_g \quad \text{for } M_b > M_s \quad (25)$$

As can be seen, for axial load factor equal to zero ($K = 0$), results derived from Eqs. (24) and (25) and Eq. (3) are quite identical. Based on mentioned equations, the neutral axis is depended on value of axial load generated by seismic actions. Therefore, moment–rotation of a RC column under varying axial load can be calculated by the mentioned procedure in the previous section and only the neutral axis should be determined using Eqs. (24) and (25). To clarify the proposed procedure for taking into account the effects of variations of axial load, the interaction between flexural, shear and axial behaviour for a value of concrete strain ϵ_c at the extreme compression fiber of section was illustrated in Fig. 6. As can be seen, by plotting flexural and shear moment versus axial load diagram, value of axial load corresponding to concrete strain $\epsilon_{c,i}$ can be computed. Moreover, to detect the failure mode of column, the flexural and shear behaviours were separately considered. Therefore, using this procedure, the axial load corresponding to each value of concrete strain at the extreme compression fiber of section, $\epsilon_{c,i}$, can be derived such that the effects of variations of axial load were considered. For columns with shear or flexural behaviour, the neutral axis and consequently, shear or flexural moment corresponding to this point can be calculated using Eqs. (24) and (25) respectively. In order to define the response of column in term of ductility, this point should be converted to moment–curvature diagram. This diagram can be plotted through the determination of

curvature corresponding to moment M_i for applied axial load N_i on column. However, according to proposed model, the nonlinear behaviour of columns were simulated by rotational springs (see Fig. 1). Therefore, to obtain properties of these springs, the moment–curvature diagram should be transformed to moment–rotation diagram. For this purpose, Eqs. (24) and (25) can be adopted for each value of curvature corresponding to the concrete strain at the extreme compression fiber of section. It should be noted that for determining the different types of the curvature distribution, namely the elastic and inelastic curvature distribution, we need to calculate the yield curvature corresponding to the yield strain, ϵ_y , in tensile reinforcements. It can be derived taking into account interaction between the yield curvature and axial load that is computed through section analysis for various applied axial load on column. Therefore, for each value N_i , the yield curvature ϕ_y can be obtained (see Fig. 6). It should be noted that using Eqs. (24) and (25), the neutral axis and consequently, strain in tensile reinforcements at any level of axial load, is obtained. Therefore, comparing obtained strain with ϵ_y , the elastic and inelastic curvature distribution can be detected. As a result, using this procedure, the moment–curvature diagram is converted to moment–rotation relation that can be assigned to rotational spring of column. In order to assess the effect of value K on the nonlinear response of RC columns, a parametric analysis was carried out on the cantilever column with 1400 mm height and $450 \times 450 \text{ mm}^2$ cross-sectional dimensions. The column longitudinal reinforcement ratio was taken into account as 2.55%. The transverse reinforcements consisted of 6-mm placed at 300 mm. A constant axial load, N_g , was taken into account as $0.2 f'_c A_g$. The compressive strength of concrete and the yield stress of steel bars were assumed 20 and 420 MPa, respectively.

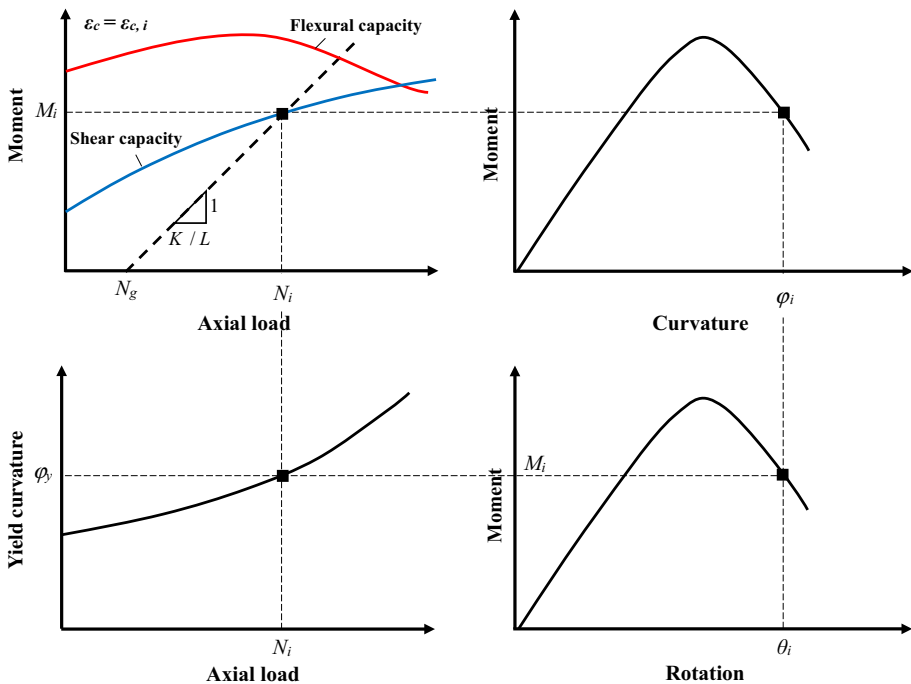
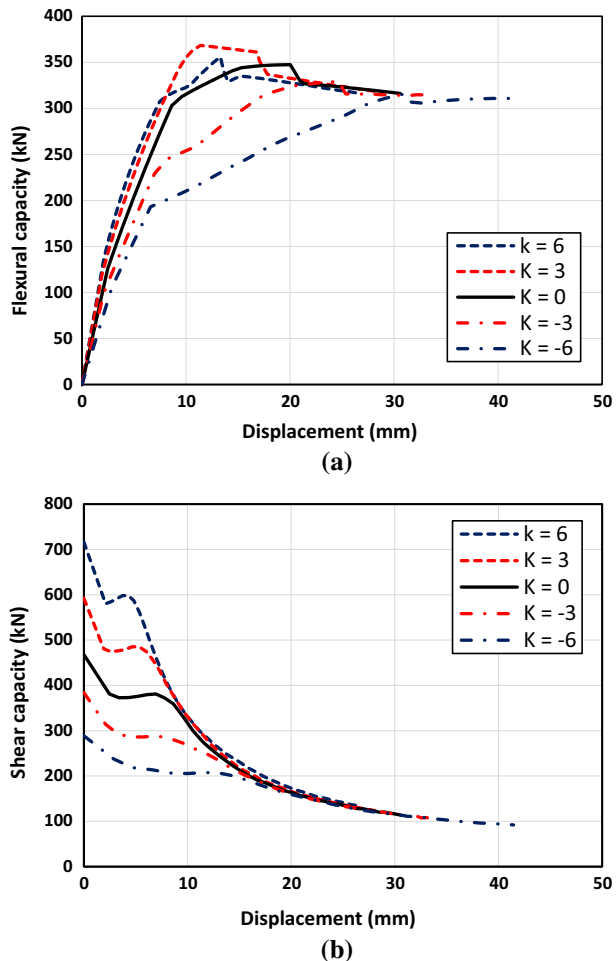


Fig. 6 Moment–rotation relation of RC column under varying axial load

In Fig. 7, the effects of variations of axial load on the flexural and shear capacities of the aforementioned column was examined. As can be observed in Fig. 7a, the initial stiffness of the column is a function of the axial load factor so that it can be positively affected increasing K from -6 to 6 . As a result, taking into account only the gravity load value in the column, N_g , the initial stiffness is estimated as misleading. It is well known that the flexural capacity of a RC column is improved increasing the level of axial load up to the balanced point (tension-controlled column) and a ductile failure for column part can be expected. On the contrary, after this point, the flexural moment is negatively affected by the axial load (compression-controlled column) and column failure mode changes to an undesirable and brittle failure mode.

Therefore, as can be seen in Fig. 7a, increasing K from -6 to 6 , initially, the maximum flexural capacity was enhanced to the balanced point (for the aforementioned column, the axial load corresponding to the balanced point is approximately $0.45 f'_c A_g$), but, at higher axial load levels, the column flexural capacity is negatively affected increasing the axial load factor. Therefore, considering $K = 0$, misleading results may be computed by

Fig. 7 Effect of axial load variations on **a** flexural behaviour **b** shear behaviour



nonlinear analysis. Figure 7b compares the shear capacity of the mentioned column under various axial load factors. As can be seen, neglecting the effect of the variations of axial load, the column shear capacity can be conservative for $K > 0$, while the same for $K < 0$ can be quite unsafe and non-conservative.

In Fig. 8, the lateral load versus displacement response of the mentioned column in various axial load factors was evaluated. Since the lateral force versus displacement response of RC columns with shear or flexural–shear behaviour is crucially dependent on the shear demand as well as the shear capacity, the axial load variations can influence nonlinear behaviour of RC columns considering the effect of axial load variations on flexural and shear capacities. As can be seen in Fig. 8, by considering $K = 0$, the response of the column in terms of initial stiffness, strength and displacement ductility leads to misleading prediction.

In Fig. 9, the effects of the axial force variations on curvature ductility factor (ϕ_f/ϕ_y) and flexural stiffness (I_e/I_g) were highlighted. As can be seen, as expected, increasing the curvature ductility factor, flexural stiffness reduces due to increasing flexural cracking. It should be noted that the curvature ductility factor of a RC column is inversely proportional to axial load factor K . Since the neutral axis is a function of parameter K [Eqs. (24) and (25)], considering a value of the normal strain, ϵ_{e_c} , at the extreme compression fiber, an increase of K induced an increase of axial load and the neutral axis which can reduce curvature ductility. According to above discussion, neglecting the effect of the variations of axial load, the assessment of the nonlinear behaviour of a RC column leads to misleading predictions. As a results, Figs. 7, 8 and 9 confirm the importance of taking into account the effect of the variations of axial load applied on column in nonlinear analyses.

5 Verification of proposed flexural and shear model at sub-assembly level

This section represents the validation of the proposed procedure for determining properties of column rotational springs. For this purpose, four columns which tested by Gill et al. (1979), Lynn (2001) and Sezen (2002) were selected.

Fig. 8 Effect of axial load variations on load–displacement relation. The *solid* and *dashed* lines represent the flexural and shear behaviours of the column, respectively

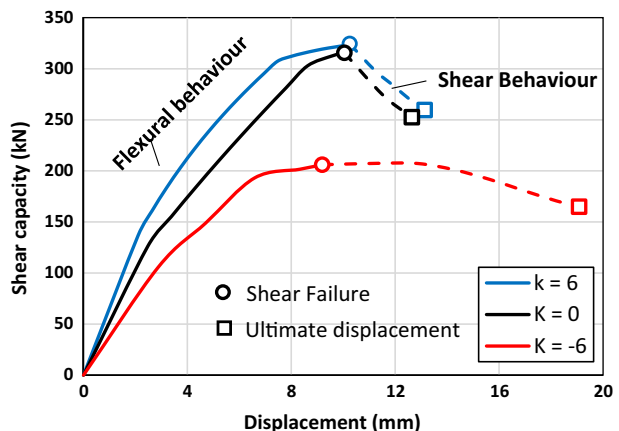
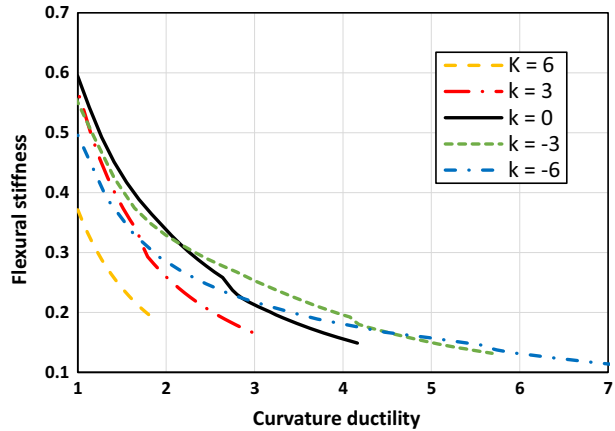


Fig. 9 Effect of axial force variations on curvature ductility factor and flexural stiffness (I_e/I_g)



5.1 Tests by Gill et al. (1979)

Gill et al. (1979) performed tests on four RC columns with various axial load. For test unit 1, test unit 2, test unit 3 and test unit 4, the concrete strength was reported as 23.1, 41.4, 21.4 and 23.5 MPa, respectively. The yield strength of 10, 12 and 24 mm diameter bars were measured as 297, 294 and 375 MPa, respectively. For test unit 1, test unit 2, test unit 3 and test unit 4, the applied axial stress on the column was reported as 26, 21, 42 and 60% of concrete compressive strength, respectively. Also, failure mode for columns tested by Gill et al. (1979) was reported as flexural failure. Complete details of tested specimens are given by Gill et al. (1979). Figure 10 describes the comparison of the load–displacement curves obtained from analytical analyses and reported from the experiments (Gill et al. 1979). As can be seen, very good agreement between experimental and analytical curves confirms the reliability of the proposed procedure for determining properties rotational springs.

5.2 Tests by Lynn (2001)

Lynn (2001) conducted tests on four RC columns with various axial load. For specimens 2SLH18, 3CLH18, 3CMD12 and 3SMD12, the concrete strength was reported as 33.1, 26.9, 27.6 and 25.5 MPa, respectively. The yield strength of 25.4 and 32.3 mm diameter reinforcements was reported as 331 MPa and the same for 9.5 mm diameter reinforcements was measured as 400 MPa. For specimens 2SLH18, 3CLH18, 3CMD12 and 3SMD12, the applied axial stress on the column was reported as 7, 9, 26 and 28% of concrete compressive strength, respectively. Also, failure mode for columns tested by Lynn (2001) was reported as shear failure. Complete details of tested specimens are given by Lynn (2001). In Fig. 11, the load–displacement curves obtained from analytical analyses and reported from the experiments (Lynn 2001) were compared. For specimens 2SLH18, 3CLH18, it can be seen that the analytical and experimental results are in a reasonably good agreement. Moreover, the ultimate displacement corresponding to 80% of the peak load occurred prior to the axial failure limit. As a result, the no axial mechanism appeared in the columns. For specimens 3CMD12 and 3SMD12, it can be seen that the experimental results were predicted by the proposed procedure with reasonable accurate. Moreover, the ultimate displacement corresponding to 80% of the peak load exceeded the

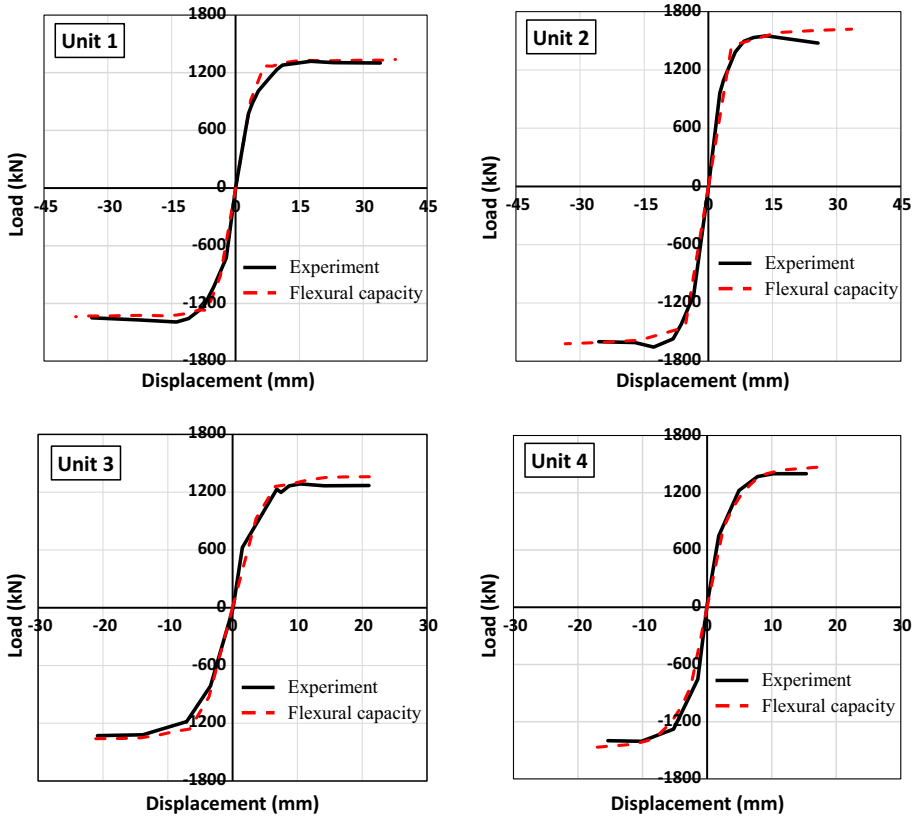


Fig. 10 Validation of proposed model for specimens tested by Gill et al. (1979)

axial failure limit. In this case, not only the effect of the column axial failure was considered but the column post peak behaviour was also modified. As a result, with regard to obtained results, in order to be conservative, the axial failure limit proposed by Elwood and Moehle (2005) can be useful.

5.3 Tests by Sezen (2002)

Sezen (2002) conducted tests on RC columns under constant and varying axial load. The chosen specimen is Specimen-3, which was tested under varying axial load. The concrete compressive strength was measured as 20 Mpa. The yield strengths of the longitudinal bars and transverse reinforcements in the tested column were reported as 441 and 469 MPa, respectively. The initial axial load on column was reported as 25% of its axial load carrying capacity and for simulating the varying axial load in a medium-rise building, the axial load factor, K , was taken as 5.83 and -4.67 for positive and negative directions, respectively. Failure mode for column tested by Sezen (2002) was reported as shear failure. Complete details of tested specimen are given by Sezen (2002). For the aforementioned column, two types of analytical analysis were carried out, one taking into account the effect of axial load variations and another neglecting this effect. Figure 12 compares the

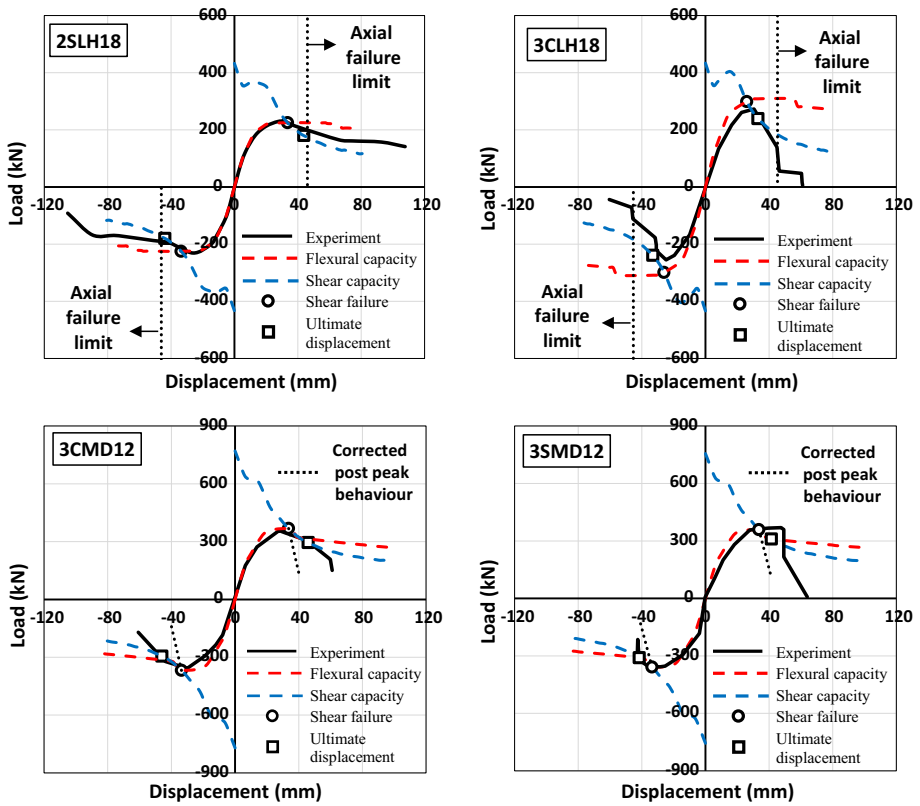


Fig. 11 Validation of proposed model for specimens tested by Lynn (2001)

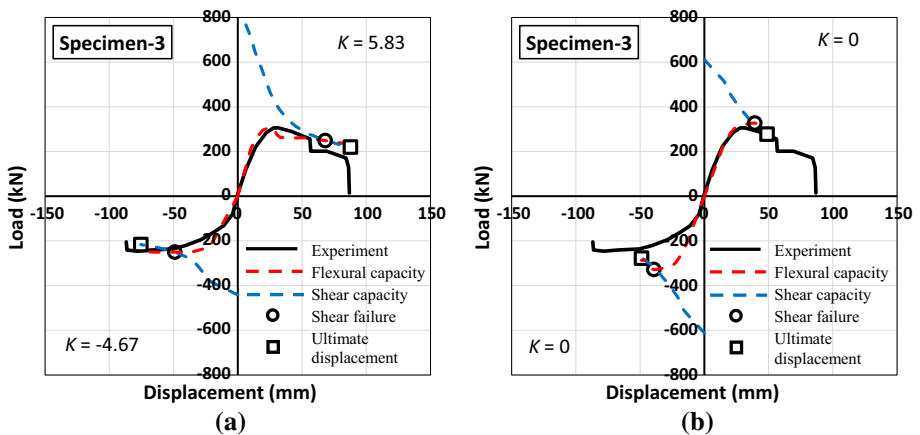


Fig. 12 Simulation of specimen tested by Sezen (2002). **a** Considering the effect of axial load variations, **b** neglecting the effect of axial load variations

load–displacement curves obtained from analytical analysis and reported from the experiment (Sezen 2002).

As can be seen, good agreement between experimental and numerical curves confirms the reliability of the proposed procedure for determining response of RC columns including shear behaviour under varying axial loading histories. On the other hand, neglecting the effect of the axial load variations, for the both positive and negative directions, a higher column strength was predicted than the analytical analysis taking into account this effect. Moreover, in case of $K = 0$, the response of RC column in term of ductility was on conservative side. As a result, the analytical analysis neglecting the effect of the axial load variations, misleading results in terms of the prediction of the seismic performance of a RC column can be obtained.

5.4 Tests by Abrams (1987)

Abrams (1987) conducted tests on four RC columns under two different axial load paths. For the specimens C4 and C8, the concrete strength was reported as 33.4 and 45.9 MPa, respectively. The yield strength of the longitudinal reinforcements was reported as 423 MPa. For the specimen C4, axial load was considered to vary in proportion to flexural moment. In order to use Eq. (23), in current study, the proportionality coefficient was converted to the axial load factor K depending on the lateral load. Therefore, K was taken into account equal to $2.63 \times L$ (L is the column height in m). Moreover, an initial axial load equal to $0.11 \times f'_c \times A_g$ was applied to the test specimen. For the specimen C8, the axial load was considered to change linearly with lateral displacement up to a maximum or minimum value corresponding to twice the yield displacement ($2\Delta_y$). At this stage, the proportionality coefficient, K' , was taken into account to equal to 13.73 kN/mm. In this study, in order to consider the effects of the variations of axial load, the natural axis can be computed by Eqs. (26) and (27), respectively.

$$\sum f_c(x)b_w t_s + \sum F_{si} - K' \times \left[\frac{\varphi_i L_{eff}^2}{3} \right] = N_g \quad \text{for } \Delta_i \leq \Delta_y \quad (26)$$

$$\sum f_c(x)b_w t_s + \sum F_{si} - K' \times \left[\frac{\varphi_y L^2}{3} + (\varphi_i - \varphi_y)L_p(L_{eff} - 0.5L_p) \right] = N_g \quad (27)$$

for $\Delta_y \leq \Delta_i \leq 2\Delta_y$

where Δ_i is the lateral displacement. For $\Delta_i > 2\Delta_y$, the axial load was considered to be constant corresponding to 575 and 45 kN for push and pull directions, respectively. Therefore, the natural axis can be determined using Eq. (3). For the specimen C8, an initial axial load equal to $0.1 \times f'_c \times A_g$ was applied to the test specimen. The failure mode for columns tested by Abrams (1987) was reported as flexural failure. Complete details of tested specimens are given by Abrams (1987). Figure 13 describes the comparison of the load–displacement curves obtained from analytical analyses and reported from the experiments (Abrams 1987). As can be seen, for the specimen C4, the analytical estimation of the load–displacement response is in reasonably good agreement with the experimental counterpart. For the specimen C8, although the axial load path considered in the analytical model match successfully with the axial load path followed in the test, the proposed analytical procedure slightly underestimated the column flexural strength and overestimated the displacement ductility capacity of the column. It is noteworthy that the specimen C8 was chosen as an example for the worst estimation.

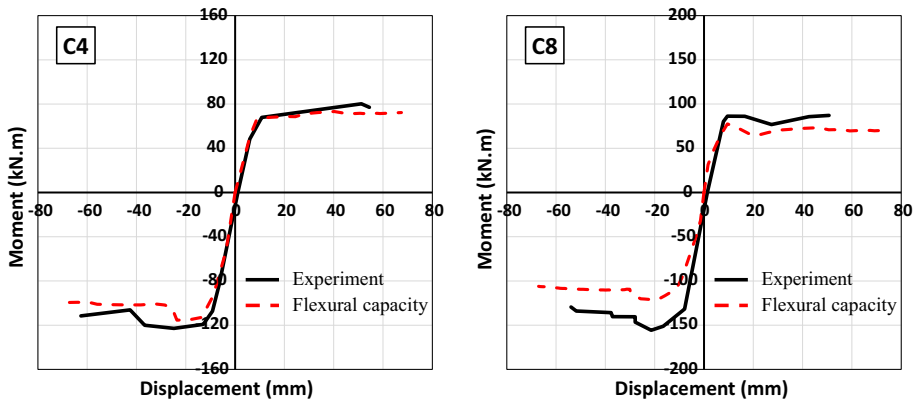


Fig. 13 Validation of proposed model for specimens tested by Abrams (1987)

6 Validation of the proposed approach at structural level

In order to assess the performance of the proposed method at structural level, two shear and flexure-critical reinforced concrete frames tested by Duong et al. (2007) and Vecchio and Emara (1992) were chosen and the results predicted by the proposed model were compared with the one captured from the experiments. The failure mode of the frame tested by Duong et al. (2007) was reported as shear failure. In this case, the pushover analysis was carried out in various cases in order to assess the importance of considering the effects of shear in RC members. On the other hand, in the flexure-critical reinforced concrete frame tested by Vecchio and Emara (1992), the ability of the proposed method to predict the flexural behaviour of the members was investigated.

6.1 Test by Duong et al. (2007)

A single-span, two-storey RC frame with a fixed base condition was tested by Duong et al. (2007). Figure 14 shows the details of the frame and the nonlinear characteristics of the plastic hinges defined by the proposed procedure. The test frame was subjected to a lateral

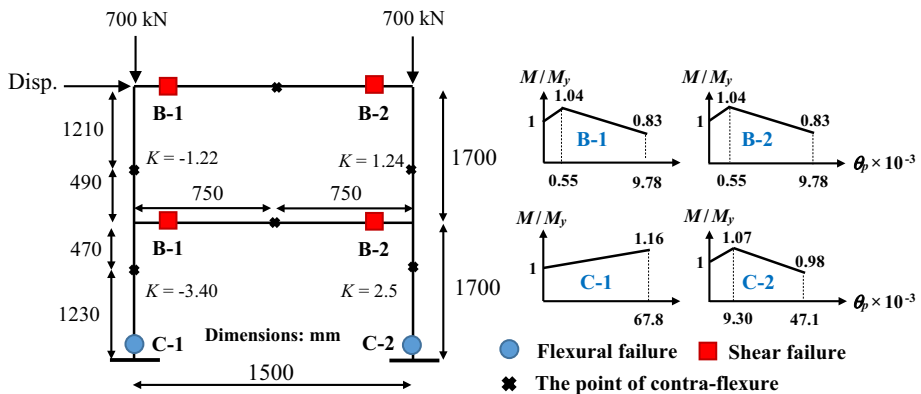


Fig. 14 The details of the frame tested by Duong et al. (2007) and failure patterns observed for the frame

displacement to the second storey beam. The concrete compressive strength was measured as 42.9 MPa. Complete details are given by Duong et al. (2007). In order to accurately assess the proposed procedure with the experiment results, two sets of settings for the rotational spring of the RC members were used in nonlinear analysis, (1) with no simulating the effects of shear with the common assumption that shear failure of the members can be neglected in the analysis, (2) simulating the shear effects adopting the procedure proposed in the current study. The comparison of numerical and experimental load–displacement curves are given in Fig. 15. A good agreement can be observed between the load–displacement curves derived from the numerical analysis and reported from the test when the shear effect was simulated.

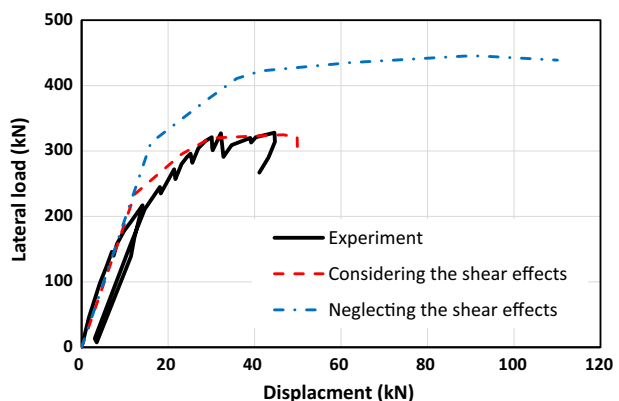
Moreover, as can be seen in Fig. 15, the response of the frame both in terms of strength and ductility is inaccurately predicted when the shear effect is not simulated. Reported failure modes, namely shear failure of the beams and flexural cracks at the column, can be successfully predicted considering the shear effects (see Fig. 14).

6.2 Test by Vecchio and Emara (1992)

A single-span, two-storey RC frame with a fixed base condition was tested by Vecchio and Emara (1992). The test frame was subjected to a lateral displacement to the second storey beam. The concrete compressive strength was reported as 30 Mpa. Figure 16 shows the details of the frame and the nonlinear characteristics of the plastic hinges defined by the proposed procedure. Even though some shear cracks were observed in the members, the frame predominantly failed in flexural. Complete details are given by Vecchio and Emara (1992). To accurately investigate the proposed pushover procedure with the experiment results, two sets of settings for the plastic hinge of the RC members were used in pushover analysis, (1) using the values recommended by the FEMA-356 guidelines (ASCE 2000) to define plastic hinges, (2) using the proposed procedure to define plastic hinges. In Fig. 17, the comparison of experimental and numerical load–displacement curves is shown. Good agreement can be observed between the load–displacement curves extracted from the numerical analysis and experimental results when the plastic hinge were defined by the proposed procedure.

Moreover, the typical failures observed in the experiment, namely flexural hinges in beams and columns can be successfully replicated in the nonlinear analysis (see Fig. 16). On the contrary, using the values recommended by the FEMA-356 guidelines (ASCE

Fig. 15 Force–displacement curve of the frame extracted from experiment (Duong et al. 2007) and obtained from numerical analysis



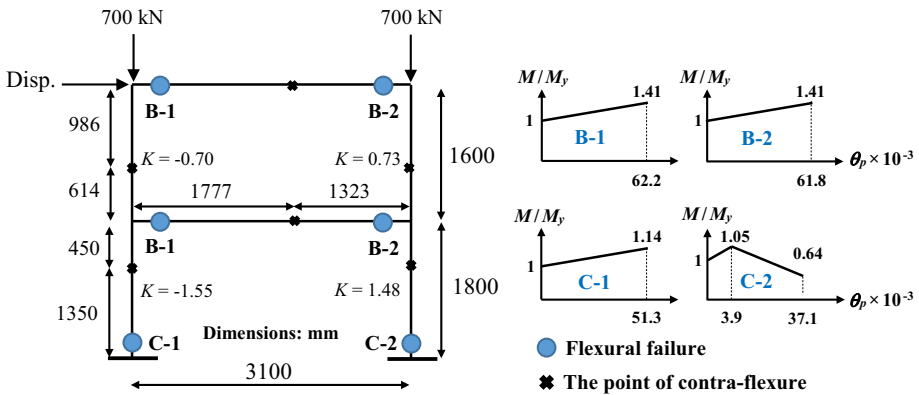


Fig. 16 The details of the frame tested by Vecchio and Emara (1992) and failure patterns observed for the frame

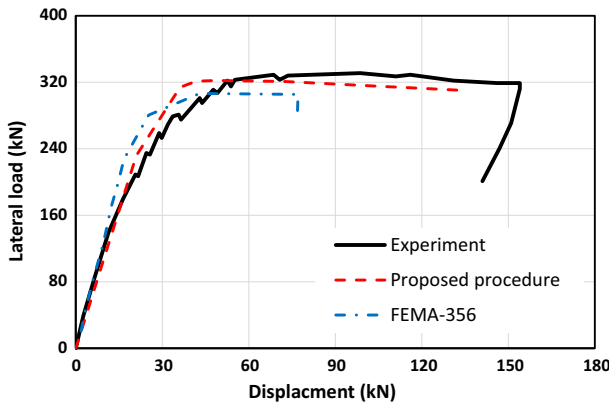


Fig. 17 Force–displacement curve of the frame extracted from experiment (Vecchio and Emara 1992) and obtained from numerical analysis

2000) for defining plastic hinge, the pushover analysis provides a conservative estimate of less than half of the displacement capacity reported from test.

7 Summary and conclusions

In current study, in order to simulate RC members taking into account flexural and shear behaviours in a numerical analysis a model including rotational springs was developed. In order to compute the nonlinear properties of RC members, moment–curvature analysis of section can be used based on the principles of strain compatibility and equilibrium and material constitutive relations for concrete and steel. Moreover, the effect of the buckling of longitudinal bars was considered in the model through controlling the ultimate rotation. According to the material failure criteria of concrete, in the compression zone of the RC cross-section, the shear capacity contribution due to concrete was determined as a function of the inelastic deformation. Moreover, the relationship between applied axial load on

column and the drift at axial failure was considered in the shear model. Considering interaction between shear and flexural behaviours, failure mode of RC beams and columns including flexural, shear–flexural and shear failure can be detected through the comparison of the values of shear and flexural moment. During earthquakes, columns, especially the exterior ones, can be subjected to variable axial loads. In order to take into account this effect, a simplified methodology was developed so that the applied axial load on the column was varied around the gravity load value proportionally to the lateral load acting on the column. The proposed analytical model was applied to experiments available in the literature at sub-assembly level under cyclic loading as well as at structural level under lateral loading. The result proved that the model is able to estimate the nonlinear behaviour of the RC members under constant or varying axial load with reasonable precision. The developed model is also suitable enough to be adopted in the software programs such as SAP2000 (2008).

A parametric analysis were also carried out in order to highlight the effect of the variations of axial load on nonlinear response of RC columns. The results showed that ignoring the axial load variation effects, the column response obtained from analytical analysis leads to misleading results in terms of predicting flexural and shear capacities, strength, deformation capacity and stiffness.

References

- Aboutaha RS, Engelhardt MD, Jirsa JO, Kreger ME (1999) Rehabilitation of shear critical concrete columns by use of rectangular steel jackets. *Am Conc Inst ACI Struct J* 96(1):68–78
- Abrams DP (1987) Influence of axial force variations of flexural behavior of reinforced concrete columns. *ACI Struct J* 84(3):246–254
- American Society of Civil Engineering (ASCE) (2000) Prestandard and commentary for the seismic rehabilitation of buildings (FEMA-356). Federal Emergency Management Agency, Washington
- Ang BG, Priestley MJN, Paulay T (1989) Seismic shear strength of circular reinforced concrete columns. *ACI Struct J* 86(1):45–59
- Applied Technology Council (ATC 32) (1996) Improved seismic design criteria for California bridges: provisional recommendations. Redwood City, CA
- Aschheim M, Moehle JP (1992) Shear strength and deformability of RC bridge columns subjected to inelastic cyclic displacements. Report No. UCB/EERC-92/04, Earthquake Engineering Research Center, University of California at Berkeley, Berkeley, CA
- Baradaran Shoraka M (2013) Collapse assessment of concrete buildings: an application to non-ductile reinforced concrete moment frames. Ph.D. dissertation, University of British Columbia, Canada
- Berry MP, Eberhard MO (2005) Practical performance model for bar buckling. *J Struct Eng* 131(7):1060–1070
- Chen WF (1982) *Plasticity in reinforced concrete*. McGraw-Hill, New York, p 474
- Colajanni P, Recupero A, Spinella N (2015) Shear strength degradation due to flexural ductility demand in circular RC columns. *Bull Earthq Eng* 13(6):1795–1807
- Computer and Structures Inc (2008) SAP2000 analysis references, Berkeley, California
- Duong KV, Sheikh SA, Vecchio FJ (2007) Seismic behavior of shear-critical reinforced concrete frame: experimental investigation. *ACI Struct J* 104(3):304–313
- ElMandooh Galal K, Ghobarah A (2003) Flexural and shear hysteretic behaviour of reinforced concrete columns with variable axial load. *Eng Struct* 25(23):1353–1367
- Elwood KJ (2004) Modelling failures in existing reinforced concrete columns. *Can J Civ Eng* 31(5):846–859
- Elwood KJ, Moehle JP (2003) Shake table tests and analytical studies on the gravity load collapse of reinforced concrete frames. Report no. PEER 2003/01. Pacific Earthquake Engineering Research Center
- Elwood KJ, Moehle JP (2005) Axial capacity model for shear-damaged columns. *ACI Struct J* 102(4):578–587

- Gill WD, Park R, Priestley MJN (1979) Ductility of rectangular reinforced concrete columns with axial load. Report 79-1, Department of Civil Engineering, University of Canterbury, Christchurch, New Zealand
- Guner S, Vecchio FJ (2011) Analysis of shear-critical reinforced concrete plane frame elements under cyclic loading. *J Struct Eng* 137(8):834–843
- Ho JCM, Pam HJ (2003) Inelastic design of low-axially loaded high-strength reinforced concrete columns. *Eng Struct* 25:1083–1096
- Kreger ME, Linbeck L (1986) Behaviour of RC columns subjected to lateral and axial load reversals. In: Proceedings of the third national conference on earthquake engineering, Charleston, South Carolina, USA, vol 2, pp 1475–1486
- Lee J-Y, Watanabe F (2003) Predicting the longitudinal axial strain in the plastic hinge regions of reinforced concrete beams subjected to reversed cyclic loading. *Eng Struct* 25:927–939
- Li KN, Aoyama H, Otani S (1988) Reinforced concrete columns under varying axial load and bi-directional lateral load reversals. In: Proceedings of ninth world conference on earthquake engineering, Tokyo-Kyoto, Japan, vol 8, pp 537–542
- Lynn A (2001) Seismic evaluation of existing reinforced concrete building columns. Ph.D., dissertation, University of California at Berkeley, Berkeley, CA
- MacGregor JG, Sozen MA, Siess CP (1960) Strength and behavior of prestressed concrete beams with web reinforcement. University of Illinois Civil Engineering Studies, Structural Research Series 210, Urbana
- Mander JB, Priestley MJN, Park R (1988) Theoretical stress–strain behavior of confined concrete. *J Struct Eng* 114(8):1804–1826
- Matchulat L (2009) Mitigation of collapse risk in reinforced concrete buildings. M.S., thesis, University of Kansas, Lawrence, KS
- Moharrami M, Koutromanos I, Panagiotou M, Girgin SC (2015) Analysis of shear-dominated RC columns using the nonlinear truss analogy. *Earthq Eng Struct Dyn* 44:677–694
- Moretti M, Tassios TP (2007) Behaviour of short columns subjected to cyclic shear displacements: experimental results. *Eng Struct* 29:2018–2029
- Mullapudi TR, Ayoub A (2010) Modeling of the seismic behavior of shear-critical reinforced concrete columns. *Eng Struct* 32:3601–3615
- Niroomandi A, Maheri A, Maheri MR, Mahini SS (2010) Seismic performance of ordinary RC frames retrofitted at joints by FRP sheets. *Eng Struct* 32(8):2326–2336
- Niroomandi A, Najafgholipour MA, Ronagh HR (2014) Numerical investigation of the affecting parameters on the shear failure of Nonductile RC exterior joints. *Eng Fail Anal* 46:62–75
- Niroomandi A, Pampanin S, Dhakal R, Soleymani Ashtiani M (2015) Comparison of alternative assessment procedures to predict seismic performance of RC columns. In: Proceedings of tenth Pacific conference on earthquake engineering, Sydney, Australia
- Ousaleh H, Kabeyasawa T, Tsasai A, Ohsugi Y (2002) Experimental study on seismic behavior of reinforced concrete columns under constant and variable axial loadings. In: Proceedings of the annual conference of Japan concrete institute, Tsukuba, Japan, vol 24, no 2, pp 229–234
- Ousaleh H, Kabeyasawa T, Tsasai A, Iwamoto J (2003) Effect of hysteretic reversals on lateral and axial capacities of reinforced concrete columns. In: Proceedings of the annual conference of Japan concrete institute, Kyoto, Japan, vol 25, no 2, pp 367–72
- Park H, Choi K, Wight JK (2006) Strain-based shear strength model for slender beams without web reinforcement. *ACI Struct J* 103(6):783–793
- Park H, Yu E, Choi K (2012) Shear-strength degradation model for RC columns subjected to cyclic loading. *Eng Struct* 34:187–197
- Paulay T, Priestley MJN (1992) Seismic design of reinforced concrete and masonry buildings. Wiley, New York
- Priestley MJN, Verma R, Xiao Y (1994) Seismic shear strength of reinforced concrete columns. *J Struct Eng* 120(8):2310–2329
- Priestley MJN, Seible F, Calvi GM (1996) Seismic design and retrofit of bridges. Wiley, New York
- Saadeghvaziri MA, Foutch DA (1990) Behavior of RC columns under non proportionally varying axial load. *J Struct Eng* 116(7):1835–1856
- Sezen H (2002) Seismic behavior and modeling of reinforced concrete building columns. Ph.D., dissertation, University of California at Berkeley, Berkeley, CA
- Sezen H, Moehle JP (2002) Seismic behavior of shear-critical reinforced concrete building columns. In: Seventh US national conference on earthquake engineering. Earthquake Engineering Research Institute, Boston, MA
- Sezen H, Moehle JP (2004) Shear strength model for lightly reinforced concrete columns. *J Struct Eng* 130(11):1703–1962

- Shayanfar J, Akbarzadeh BH (2016) Numerical model to simulate shear behaviour of RC joints and columns. *Comput Concr*. doi:[10.12989/cac.2016.18.6.000](https://doi.org/10.12989/cac.2016.18.6.000)
- Shayanfar J, Akbarzadeh BH, Niroomandi A (2016) A proposed model for predicting nonlinear behavior of RC joints under seismic loads. *Mater Des* 95:563–579
- Taucer F, Spacone E, Filippou FC (1991) A fiber beam-column element for seismic response analysis of reinforced concrete structures. Report no UCB/EERC 91-17. University of California, Berkeley, CA
- Vecchio FJ, Emara MB (1992) Shear deformations in reinforced concrete frames. *ACI Struct J* 89(1):46–56
- Willams MS, Sexsmith RG (1995) Seismic damage indices for concrete structures: a state-of-the-art review. *Earthq Spectra* 11(2):319–349
- Wong YL, Paulay T, Priestley MJN (1993) Response of circular reinforced concrete beams to multi-directional seismic attack. *ACI Struct J* 90(2):180–191